Acta Cryst. (1972). A**28**, 319

The Normalization of the Resolution Function for Inelastic Neutron Scattering and its Application*

BY B. DORNER

Brookhaven National Laboratory, Upton, New York 11973, *U.S.A.*
and
Institut für Festkörperforschung KFA-Jülich, Germany (BRD)†

(*Received* 18 *November* 1971)

By extending the considerations of Maier-Leibnitz, the normalization of the resolution function is found to be the product of the volumes in reciprocal space of the incident and scattered beams. Each volume is defined by an integration in reciprocal space over the probability of finding a particular **k**, where **k** is the wave vector of the neutron. The resolution can be understood as a convolution of these two volumes. For three-axis spectrometers explicit expressions for these volumes are given. The knowledge of the normalization is necessary for numerical unfolding of experimental data. For two cases, which often occur in inelastic neutron scattering, it is possible to directly correct the experimental data without resorting to numerical unfolding. After applying these corrections the data represent the scattering law folded with a resolution function normalized to unity, *i.e.* the integral over the corrected data is the integral over the scattering law. It is shown that in this case, the unfolding of the corrected data turns out to be a one-dimensional problem.

1. Introduction

The resolution function of an instrument for inelastic neutron scattering depends on the wave vectors $\mathbf{k}_i$ and $\mathbf{k}_f$ of the incoming and scattered neutrons respectively. In the Gaussian approximation‡ the surfaces of equal probability are four-dimensional ellipsoids. For a nominal setting $\mathbf{Q}_0$ and ω_0 of the instrument the resolution function R can be written

$$R(\mathbf{Q}-\mathbf{Q}_0, \omega-\omega_0) = R_0(\mathbf{Q}_0, \omega_0) \times \exp\left\{-\tfrac{1}{2}\sum_{k=1}^{4}\sum_{l=1}^{4} M_{kl}(\mathbf{Q}_0, \omega_0)X_kX_l\right\}. \quad (1)$$

Here $\hbar\mathbf{Q}=\hbar\mathbf{k}_i-\hbar\mathbf{k}_f$ is the momentum transfer and $\hbar\omega = \frac{\hbar^2}{2m}(k_i^2-k_f^2)$ the energy transfer. $\hbar\mathbf{Q}_0$ and $\hbar\omega_0$ represent the most probable momentum and energy transfers and are defined in terms of the most probable values $\mathbf{k}_I$ and $\mathbf{k}_F$ of $\mathbf{k}_i$ and $\mathbf{k}_f$. The matrix $\mathbf{M}_{kl}$ describes the ellipsoids and the four coordinates X_k represent the three components of $(\mathbf{Q}-\mathbf{Q}_0)$ and $\omega-\omega_0$. The semi-major axes of these ellipsoids have been derived for a three-axis spectrometer by Stedman & Nilsson (1966), Cooper & Nathans (1967), Stedman (1968), Nielsen & Bjerrum Møller (1969) and Bjerrum Møller & Nielsen (1970) and for a time-of-flight instrument by Komura & Cooper (1970). But the efficiency factor $R_0(\mathbf{Q}_0, \omega_0)$ and the normalization (by which we mean the integral over R) have not yet been discussed in the literature, although they play an important role in resolution corrections. For example, failure to take the normalization into consideration in analyzing experimental data can cause errors in the determination of both peak positions and line shapes. Integrated intensities, which are of increasing interest in inelastic neutron scattering measurements also depend crucially on the normalization.

In this paper a general and surprisingly simple expression for the normalization of the resolution is derived by extending Maier-Leibnitz's (1966) treatment of intensity and resolution in neutron scattering. Tucciarone, Lau ,Corliss, Delapalme & Hastings (1971) have also considered the question of normalizing resolution calculations. Their results are in agreement with those reported here after taking into account an improper normalization§ in Cooper & Nathans' original paper. Nevertheless, in practice this error is

* Work performed under the auspices of the U. S. Atomic Energy Commission.

† Permanent address.

‡ By Gaussian approximation, we mean that Gaussian distributions are used for all quantities which determine the properties of the neutron beams, such as collimators, mosaic widths, pulse lengths, energy widths, counter thicknesses, *etc.*

§ In the course of deriving the normalization we discovered an error in formula (24) of Cooper & Nathans. This is discussed in Appendix I.

relatively minor and a computer program based on these considerations has been used to successfully analyze experimental data in the Brookhaven group for several years (Samuelsen, Hutchings & Shirane, 1970; Lau, Corliss, Delapalme, Hastings, Nathans & Tucciarone, 1970; Als-Nielsen, Axe & Shirane, 1971; Hutchings, Shirane, Birgeneau & Holt, 1971). This program and another one written by Hutchings and Samuelsen (1970), which also uses the erroneous expression of Cooper & Nathans (Samuelsen, 1972), were found in good agreement with calibration measurements of phonons in copper (Shirane, 1971). Werner & Pynn's (1971) calculations of corrections for resolution effects follow a different approach and do not give an explicit normalization. Numerical integration was checked to agree with the normalization given here (Werner, 1971).

The authors cited in the last paragraph have only considered resolution effects in three-axis spectrometers. Dietrich (1971) has treated the analogous problem for a time-of-flight spectrometer and has derived not only the parameters of the resolution function but the normalization as well.

The paper is organized in the following way. In Section 2 the counting rate at the detector is calculated following the 'phase space' considerations of Maier-Leibnitz. This approach is the key to a transparent interpretation of the normalization of the resolution function, which is derived in Section 3. An explicit expression of the normalization for a three-axis spectrometer is given in Section 4. In Section 5 we discuss the corrections to experimental data obtained with a three-axis spectrometer and in Section 6 we show that by using the Gaussian approximation in calculating the resolution function the unfolding of the data often becomes a one-dimensional problem.

2. The neutron counting rate at the detector

From equations (5) and (7) of Maier-Leibnitz we get the infinitesimal current incident on the sample

$$\mathrm{d}J_i = A'(k_i) \,.\, \mathrm{d}F \,.\, k_i \,.\, p_i(\mathbf{k}_i) \,.\, \mathrm{d}k_{ix} \,.\, \mathrm{d}k_{iy} \,.\, \mathrm{d}k_{iz} \,, \quad (2)$$

where $\mathrm{d}F$ is an element of the geometric beam cross section. For a sample small compared to the beam area, the current can be assumed constant and $\mathrm{d}F$ can be integrated to F, which is the area of the sample. $p_i(\mathbf{k}_i)$ is the probability of finding a neutron with wave vector $\mathbf{k}_i$ in the beam produced by any monochromator and incident on the sample. $p_i(\mathbf{k}_i)$ replaces the quantity f_o used by Maier-Leibnitz.

Under the assumption of a Maxwell distribution in the reactor we write

$$A'(k_i) = \frac{\varphi}{2\pi k_T^4} \exp\left(-\frac{k_i^2}{k_T^2}\right),$$

where φ is the thermal flux in the reactor, $k_T = \left[\frac{2m}{\hbar^2} k_B T\right]^{1/2}$, k_B is the Boltzmann constant and T the effective temperature of the moderator. Fig. 1 shows schematically the scattering in real and in reciprocal space.

The scattering cross section of the sample is

$$\frac{\mathrm{d}^2\Sigma}{\mathrm{d}\Omega \mathrm{d}\omega} = N \frac{k_f}{k_i} S(\mathbf{Q},\omega) \,. \quad (3)$$

Σ is the macroscopic scattering cross section *i.e.* the scattering probability per cm and per unit area of the sample and N is the density of unit cells in the sample By equation (3) we define a scattering law $S(\mathbf{Q},\omega)$, which contains the scattering lengths of all nuclei in the sample.

In order to derive the infinitesimal current at the detector we use elements of the scattered beam in units,

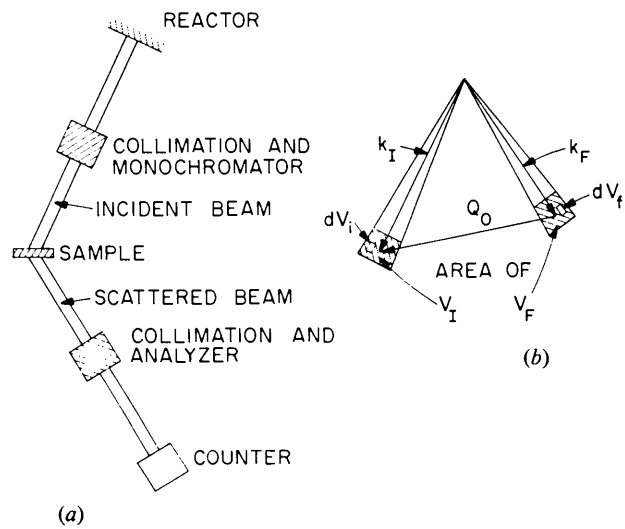

Fig. 1. Schematic drawing of an inelastic neutron scattering experiment: (*a*) in real space, (*b*) in reciprocal space.

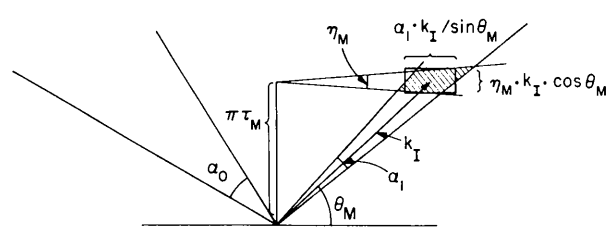

Fig. 2. Distribution of monochromatic neutrons in the scattering plane produced by a single crystal monochromator, where θ_M is the Bragg angle, $2\pi\tau_M$ the rec. lattice vector of the reflecting planes, α_0 and α_1 are the horizontal collimations of the incoming and outgoing beams and η_M is the horizontal mosaic width of the crystal.

which are compatible with the cross section given in equation (3). These elements are

$$d\Omega_f = \frac{dk_{fx} \cdot dk_{fy}}{k_f^2}, \quad d\omega_f = \frac{\hbar}{m} k_f dk_{fz}.$$

Let $p_f(\mathbf{k}_f)$ be the probability that a neutron with wave vector k_f passes the analyzer and is counted at the detector. Then for a sample of thickness t the infinitesimal current detected is

$$\begin{aligned} dJ' &= dJ_i \cdot \frac{d^2\Sigma}{d\Omega d\omega} \cdot t \cdot p_f(\mathbf{k}_f) \cdot d\Omega_f \cdot d\omega_f \\ &= A \cdot S(\mathbf{Q},\omega) \cdot p_i(\mathbf{k}_i) \cdot p_f(\mathbf{k}_f) \cdot dk_{ix} \cdot dk_{iy} \cdot dk_{iz} \\ &\times dj_{fx} \cdot dk_{fy} \cdot dk_{fz} \end{aligned} \tag{4}$$

where A includes among other factors $A'(k_i)$, t and the sample area F. By substituting

$$\begin{aligned} dV_i &= dk_{ix} \cdot dk_{iy} \cdot dk_{iz} \\ dV_f &= dk_{fx} \cdot dk_{fy} \cdot dk_{fz} \end{aligned} \tag{5}$$

in equation (4) one sees that the infinitesimal current at the detector is proportional to the volume elements in k space for the incoming and outgoing beam, as Maier-Leibnitz has shown.

Equation (4) is not as simple as it appears since the scattering law depends on $\mathbf{Q}$ and ω, while the independent variables in equation (4) are $\mathbf{k}_i$ and $\mathbf{k}_f$. Therefore, we collect all combinations of $\mathbf{k}_i$ with $\mathbf{k}_f$, which contribute to a given $\mathbf{Q}$ and ω, and write dJ proportional to elements in $\mathbf{Q},\omega$ space;

$$\begin{aligned} dJ = A \cdot S(\mathbf{Q},\omega) \int\int p_i(\mathbf{k}_i) \cdot p_f(\mathbf{k}_f) \cdot \delta[\mathbf{Q}-(\mathbf{k}_i-\mathbf{k}_f)] \\ \times \delta\left[\omega - \frac{\hbar}{2m}(k_i^2-k_f^2)\right] \cdot dV_i \cdot dV_f \cdot d^3Q \cdot d\omega. \end{aligned} \tag{6}$$

Both dJ and dJ' have the dimension neutrons per sec. Although $\int dJ' = \int dJ$, dJ' is defined in elements of $\mathbf{k}_i \cdot \mathbf{k}_f$ whereas dJ is written for elements of $\mathbf{Q}$ and ω. The δ functions in (6) represent conservation of momentum and energy. We can rewrite equation (6) in a more condensed form

$$dJ = A \cdot S(\mathbf{Q},\omega) \cdot R'(\mathbf{Q},\omega) \cdot d^3Q \cdot d\omega \tag{7}$$

where the scattering law $S(\mathbf{Q},\omega)$ describes the physical characteristics of the sample and $R'(\mathbf{Q},\omega)$ the transmission or resolution function of the instrument. A particular setting of the instrument can be described by the most probable values $\mathbf{k}_I$ and $\mathbf{k}_F$ or preferably by $\mathbf{Q}_0$ and ω_0. The resolution function $R'(\mathbf{Q},\omega)$ can be redefined in terms of $\mathbf{Q}_0$ and ω_0

$$\begin{aligned} R'(\mathbf{Q},\omega) &\equiv R(\mathbf{Q}-\mathbf{Q}_0, \omega-\omega_0) \\ &= \int\int \delta\left[(\mathbf{Q}-\mathbf{Q}_0) - \left\{\mathbf{k}_i-\mathbf{k}_f-(\mathbf{k}_I-\mathbf{k}_F)\right\}\right] \\ &\times \delta\left[(\omega-\omega_0) - \frac{\hbar}{2m}\left\{\mathbf{k}_i^2-\mathbf{k}_f^2-(\mathbf{k}_I^2-\mathbf{k}_F^2)\right\}\right] \\ &\times p_i(\mathbf{k}_i) \cdot p_f(\mathbf{k}_f) \cdot dV_i \cdot dV_f \cdot \end{aligned} \tag{8}$$

Thus the counting rate at the detector for a position $\mathbf{Q}_0$, ω_0 is given by the expression

$$J(\mathbf{Q}_0,\omega_0) = A \int S(\mathbf{Q},\omega) \cdot R(\mathbf{Q}-\mathbf{Q}_0, \omega-\omega_0) d^3Q d\omega \cdot \tag{9}$$

Note that our definition of the resolution function R differs from that of Cooper & Nathans by the factor k_f/k_i, which we have included. This definition has two advantages; first, R is now easier to understand as explained in the next section and second, the integration in equation (9) is performed over the most suitable variables, $\mathbf{Q}$ and ω. As for scattering of thermal neutrons the scattering law $S(\mathbf{Q},\omega)$ depends only on the momentum transfer $\hbar\mathbf{Q}$ and the energy transfer $\hbar\omega$ and does not depend on the chosen pair of k_i and k_f, an integration over these latter quantities as performed by Collins (1963) is unnecessarily complicated and obscures the clear separation of sample from instrumental properties as shown in equation (9).

3. The resolution function

To visualize the resolution function, it is convenient to show that R as a function of $\mathbf{Q}$ is a convolution of the probability p_i with the probability p_f. Therefore we integrate $R'(\mathbf{Q},\omega)$ [see equations (6) and (7)] over ω and obtain

$$\begin{aligned} R''(\mathbf{Q}) &= \int R'(\mathbf{Q},\omega) d\omega \\ &= \int_{V_I}\int_{V_F} \delta\left[\mathbf{Q}-(\mathbf{k}_i-\mathbf{k}_f)\right] \cdot p_i(\mathbf{k}_i) \cdot p_f(\mathbf{k}_f) \cdot dV_i \cdot dV_f \cdot \end{aligned} \tag{10}$$

The probabilities p_i and p_f describe only neutrons traveling in the direction of the beam. When k_z is negative (z being the direction of the beam) p_i and p_f are zero. This enables us to integrate from $-\infty$ to $+\infty$. The integration of equation (10) is equivalent to a projection of R' onto the $\omega=0$ plane (see Section 6).

After integration over V_F we have

$$R''(\mathbf{Q}) = \int_{V_I} p_i(\mathbf{k}_i)\, p_f(\mathbf{k}_i-\mathbf{Q})\, dV_i \tag{11}$$

which shows that $R''(\mathbf{Q})$ is a convolution of the distri-

bution of $\mathbf{k}_i$ within V_I with the distribution of $\mathbf{k}_f$ within V_F.

Alternatively, if we integrate $R'(\mathbf{Q},\omega)$ over $\mathbf{Q}$ we get

$$R'''(\omega)=\int R'(\mathbf{Q},\omega)\mathrm{d}^3Q$$
$$=\int_{V_I}\int_{V_F}\delta\left[\omega-\frac{\hbar}{2m}(k_i^2-k_f^2)\right]$$
$$\times\, p_i(\mathbf{k}_i)\,.\,p_f(\mathbf{k}_f)\,.\,\mathrm{d}V_i\,.\,\mathrm{d}V_f\,. \qquad (12)$$

The problem here is that the δ-function is a condition on the energy, which means that it selects particular combinations of k_i^2 and k_f^2, whereas the integration is performed in k-space, that is with equal steps in k.

First we define a new quantity prob(k_z) obtained by integrating over k_x and k_y. k_z is parallel to the most probable $\mathbf{k}$ ($\mathbf{k}_I$ or $\mathbf{k}_F$)

$$\text{prob}\,(k_z)=\int p(\mathbf{k})\,\mathrm{d}k_x\,\mathrm{d}k_y\,. \qquad (13)$$

After integration of equation (12) over the x and y components and $\mathrm{d}k_{fz}$ we get

$$R'''(\omega)=\int \text{prob}_i\,(k_{iz})\,.\,\text{prob}_f\left[\sqrt{\left(k_{iz}^2-\frac{2m}{\hbar}\omega\right)}\right]\mathrm{d}k_{iz}\,. \qquad (14)$$

While previously p was defined to be non-zero only when k_z is positive, now we must define prob $(\sqrt{k_z^2})$ to be non-zero only for positive k^2. Again we can integrate from $-\infty$ to $+\infty$. It is easily seen that equation (14) turns out to be a convolution in energy

$$R'''(\omega)=\int \text{prob}_i\,(\sqrt{k_{iz}^2})\,.\,\text{prob}_f\left[\sqrt{\left(k_{iz}^2-\frac{2m}{\hbar}\omega\right)}\right]$$
$$\times\,\frac{1}{2k_{iz}}\,\mathrm{d}(k_{iz})\,. \qquad (15)$$

But equation (15) is not just a convolution of the probabilities of finding a particular k_{iz} or a k_{fz}, but rather the convolution of the probabilities weighted by $1/k_{iz}$. Another interpretation is that (15) is a convolution of the two probabilities with respect to energy, but the step width is weighted to get equal steps in k space rather than in k^2 or energy space.

The properties of the resolution function discussed so far in this section are intended to help visualize the contributions from various components. We will make use of this convolution consideration in Section 5.

Let us now turn to the very important question of normalization. This requires that we integrate equation (10) over $\mathbf{Q}$

$$\int\int R'(\mathbf{Q},\omega)\,\mathrm{d}^3Q\mathrm{d}\omega=\int\int R(\mathbf{Q}-\mathbf{Q}_0,\,\omega-\omega_0)\mathrm{d}^3Q\mathrm{d}\omega$$
$$=\int_{V_I}\int_{V_F}p_i(\mathbf{k}_i)\,.\,p_f(\mathbf{k}_f)\,\mathrm{d}V_i\mathrm{d}V_f=V_I\,.\,V_F \qquad (16)$$

with

$$\int_{V_I}p_i(\mathbf{k}_i)\,\mathrm{d}V_i=V_I$$

and (17)

$$\int_{V_F}p_f(\mathbf{k}_f)\,\mathrm{d}V_f=V_F\,.$$

The normalization is proportional to the product of the volumes [as defined by (17)] in reciprocal space: V_I around $\mathbf{k}_I$ and V_F around $\mathbf{k}_F$, and is independent of the scattering angle. *Equation* (16) *contains no approximations* and holds for three-axis spectrometers as well as for time-of-flight instruments.

4. The volumes V_I and V_F for single-crystal systems

From the derivation given in the Appendix, we find

$$V_I=P_M(k_I)\,.\,k_I^3\,.\,\cot\theta_M\,.\,(2\pi)^{3/2}$$
$$\times\,\frac{\beta_0\beta_1}{\sqrt{(4\sin^2(\theta_M)\eta_M'^2+\beta_0^2+\beta_1^2)}}$$
$$\times\,\frac{\eta_M\,.\,\alpha_0\,.\,\alpha_1}{\sqrt{(\alpha_0^2+\alpha_1^2+4\eta_M^2)}} \qquad (18a)$$

$$V_F=P_A(k_F)\,.\,k_F^3\,.\,\cot\theta_A\,.\,(2\pi)^{3/2}$$
$$\times\,\frac{\beta_2\,.\,\beta_3}{\sqrt{(4\sin^2(\theta_A)\,\eta_A'^2+\beta_2^2+\beta_3^2)}}$$
$$\times\,\frac{\eta_A\,.\,\alpha_2\,.\,\alpha_3}{\sqrt{(\alpha_2^2+\alpha_3^2+4\eta_A^2)}}\,. \qquad (18b)$$

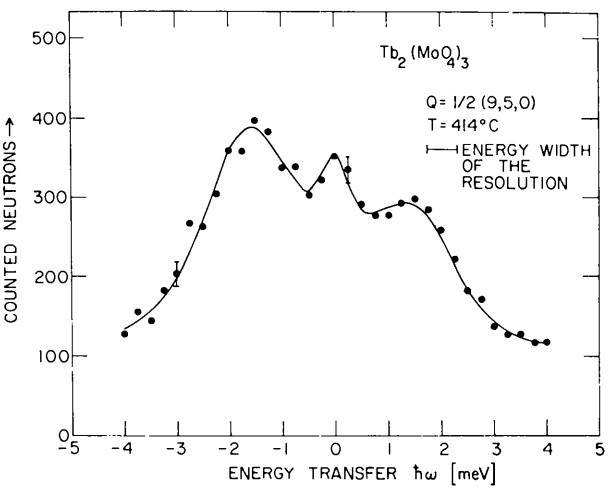

Fig. 3. Inelastic neutron scattering results of $Tb_2(MoO_4)_3$. The solid line represents a least-squares fit of a symmetric scattering law multiplied with the normalization of the resolution function.

α_0, α_1, α_2, α_3 and β_0, β_1, β_2, β_3 are the horizontal and vertical divergencies of the collimators, where 0, 1, 2, 3 refer to inpile, monochromator-to-sample, sample-to-analyzer and analyzer-to-detector respectively, η_M, η'_M, and η_A, η'_A are the horizontal and vertical mosaic widths of the monochromating and analyzing crystals respectively and θ_M, θ_A are the Bragg angles of monochromator and analyzer.

In many cases $[4 \sin^2(\theta_M)\eta'^2_M]$ can be neglected compared to $(\beta_0^2+\beta_1^2)$. Further, if $P_M(k_I)$ and $P_A(k_F)$ are assumed to be constant, one gets

$$V_I \propto k_I^3 \,.\, \cot\theta_M \tag{19a}$$

$$V_F \propto k_F^3 \,.\, \cot\theta_A \,. \tag{19b}$$

It is easy to understand relations (19*a*) and (19*b*) by referring to Fig. 2 which shows V_I projected onto the scattering plane for $\alpha_0 > \alpha_1$. The projection of V_I is proportional to $(\eta_M \,.\, k_I \,.\, \cos\theta_M) \,.\, (\alpha_1 \,.\, k_I/\sin\theta_M)$. For $\beta_0 > \beta_1$ the vertical contribution (normal to the plane of the Fig. 2) gives a factor $k_I \,.\, \beta_1$. It then follows that

$$V_I \simeq k_I^3 \,.\, \frac{\cos\theta_M}{\sin\theta_M} \,.\, \eta_M \,.\, \alpha_1 \,.\, \beta_1 \,.$$

Besides $P_M(k_I)$ and $P_A(k_F)$, η_M, η'_M, η_A and η'_A also depend on k_I and k_F respectively (Dorner, 1971) but the dependence on the wave vector can be measured and incorporated empirically into the expressions (18*a*) and (18*b*).

The above expressions for V_I and V_F contain no additional approximations beyond those made by Cooper & Nathans, *i.e.* the widths of $p_i(\mathbf{k}_i)$ and $p_f(\mathbf{k}_f)$ are small compared to $\mathbf{k}_I$ and $\mathbf{k}_F$ respectively and Gaussian distributions representing collimators and mosaic widths.

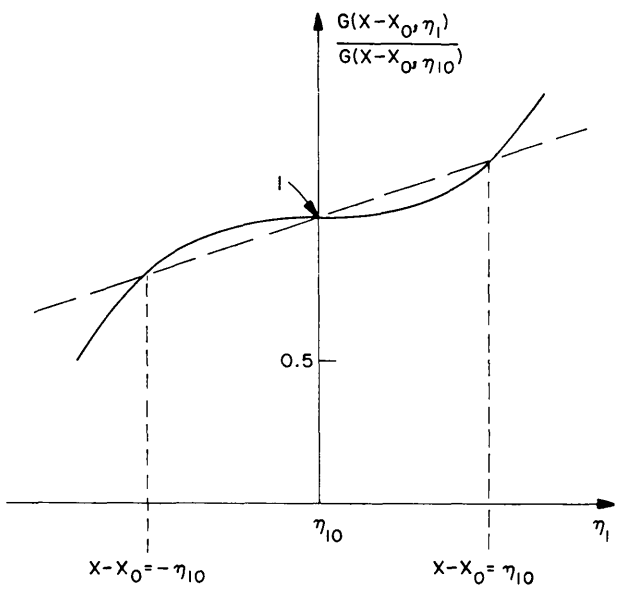

Fig. 4. The solid line represents the true effect of the resolution for varying η_1 and the broken line gives the approximation discussed in Section 5.

5. Intensity corrections for resolution effects

In Section 3 the resolution function has been derived as a property of the measuring instrument. In other words, $R(\mathbf{Q}-\mathbf{Q}_0, \omega-\omega_0)$ describes the characteristics of the instrument at a nominal position $\mathbf{Q}_0, \omega_0$. In this section, we are going to combine the characteristics of the sample, given by $S(\mathbf{Q},\omega)$, with the resolution function R. From equation (9) we see that the counting rate J is a folding of S and R. There is a complication in that the four-dimensional Gaussian R has different widths and heights at different $\mathbf{Q}_0$ and ω_0, as can be seen from equation (1). If we diagonalize the matrix $M_{kl}(\mathbf{Q}_0,\omega_0)$ to $M'_{kl}(\mathbf{Q}_0,\omega_0)$, then we can find the widths $w_k(\mathbf{Q}_0,\omega_0)$ in the directions of the four principal axes by using the relation

$$\tfrac{1}{2}M'_{kl}(\mathbf{Q}_0,\omega_0) = \frac{1}{w_k^2(\mathbf{Q}_0,\omega_0)}\,\delta_{kl} \,. \tag{20}$$

We integrate equation (1) and use equations (16) and (20) to obtain

$$\int R(\mathbf{Q}-\mathbf{Q}_0, \omega-\omega_0)\,\mathrm{d}^3Q\mathrm{d}\omega = R_0(\mathbf{Q}_0,\omega_0)\pi^2 \,.\, \prod_{k=1}^{4} w_k(\mathbf{Q}_0,\omega_0) = V_I \,.\, V_F \,. \tag{21}$$

The efficiency factor R_0 now can be expressed in terms of the normalization and the widths

$$R_0(\mathbf{Q}_0,\omega_0) = \frac{V_I \,.\, V_F}{\pi^2 \,.\, \prod_{k=1}^{4} w_k(\mathbf{Q}_0,\omega_0)} \,. \tag{22}$$

As mentioned in the introduction, the w_k for a three-axis spectrometer have been calculated by several authors. V_I and V_F for such an instrument are given in Section 4 of this paper. Hence equation (22) fully determines $R_0(\mathbf{Q}_0,\omega_0)$.

R_0 is the quantity which we must have in order to numerically integrate equation (9), *i.e.* to fold our resolution function with the scattering law. There are however two situations which are commonly encountered in inelastic neutron scattering measurements in which it is *not* necessary to do the numerical integration when the product $V_I \,.\, V_F$ is known. Let us consider these in more detail.

(*a*) $S(\mathbf{Q},\omega)$ *slowly varying in all four dimensions*

By slowly varying we mean that S varies linearly within the resolution volume. Then, since R (within Gaussian approximation) is an even function, $S(\mathbf{Q},\omega)$ can be replaced by $S(\mathbf{Q}_0,\omega_0)$ and with the help of (16) and (17) equation (9) reduces to

$$J(\mathbf{Q}_0,\omega_0) = AS(\mathbf{Q}_0,\omega_0) \,.\, V_I \,.\, V_F \,. \tag{23}$$

Thus fitting a theoretical $S(\mathbf{Q}_0,\omega_0)$ to $J(\mathbf{Q}_0,\omega_0)$ involves only multiplying S by $V_I \,.\, V_F$ and it is not necessary to unfold the data in this case. This method has been used to analyze results on quartz (Bauer, Jagodzinski, Dorner & Grimm, 1971).

As an illustrative example, we have applied equation (23) to inelastic neutron scattering data from $Tb_2(MoO_4)_3$ as described by Axe, Dorner & Shirane (1971). This is shown in Fig. 3. The scattering law, which describes a heavily damped phonon of a soft mode, is, to a good approximation, linear within the resolution volume. Moreover, the temperature is high enough compared to the energy transfers so that the scattering law can be taken to be symmetric for energy gain and loss. Therefore, the asymmetry in Fig. 3 is entirely due to the normalization of the resolution function. A least-squares fit using equation (23) gives excellent agreement with the experimental data.

(b) $S(\mathbf{Q},\omega)$ planar in four-dimensional space

By planar we mean that (i) $S(\mathbf{Q},\omega)$ is restricted in the dimension perpendicular to a plane, (ii) $S(\mathbf{Q},\omega)$ is not curved within the resolution volume. For harmonic phonons with infinite lifetime the plane, which represents the dispersion surface, has effectively zero thickness, and this can be expressed by means of a δ-function. When scanning through such an $S(\mathbf{Q},\omega)$ one has to consider the variation of two quantities, the efficiency factor R_0 and the shape of the resolution function. The shape is given by the widths w_k. We assume that the orientations of the principal axes of R do not change during the scan.

We must now consider how much of the change in the normalization $V_I \,.\, V_F$ along the scan is due to a change in the efficiency factor and how much is due to changes in the widths. To do this, we must refer back to equation (11), where we showed that at least as far as the $\mathbf{Q}$ dependence is concerned, R is a convolution of $p_i(k_i)$ with $p_f(k_f)$. Simplifying, we describe both p_i and p_f by one-dimensional Gaussians with widths η_1 and η_2 respectively. The folding of these two Gaussians $G(x)$ now represents the resolution function R. In this expression x stands for the four dimensions of R. Later, x will represent only the dimension perpendicular to the plane representing S.

$$G(x-x_0) \sim \frac{\eta_1 \,.\, \eta_2}{\sqrt{(\eta_1^2+\eta_2^2)}} \,.\, \exp\left[-\frac{(x-x_0)^2}{2(\eta_1^2+\eta_2^2)}\right]. \quad (24)$$

$$\int G(x-x_0)\,\mathrm{d}x \sim \eta_1 \,.\, \eta_2 \equiv \text{normalization}$$

$$\frac{\eta_1 \,.\, \eta_2}{\sqrt{(\eta_1^2+\eta_2^2)}} \equiv \text{efficiency factor} \sim \frac{\text{normalization}}{\text{width}}$$

Let us assume $\eta_1^2 \gg \eta_2^2$ or in other words that p_i is much wider than p_f. Then the width of $G(x)$ is entirely determined by η_1 and the efficiency factor is η_2

$$G(x-x_0) \underset{\eta_1^2 \gg \eta_2^2}{\sim} \eta_2 \,.\, \exp\left\{-\frac{(x-x_0)^2}{2\eta_1^2}\right\}. \quad (25)$$

An inelastic scan can be made either by varying k_f and holding k_I fixed or *vice versa*. The first possibility, *i.e.* k_I fixed, implies that η_1 is fixed. Hence, the width of the resolution is unchanged, during the scan and the 'overlapping' of S and R is the same on both sides of the maximum. Only the efficiency factor η_2 varies. Dividing the data at each point by η_2 (which in effect is dividing by V_F) is equivalent to a representation in which the scattering law S is folded with a normalized resolution function (see section 6).

A second possibility is that η_2 be fixed while η_1 varies. This is more complicated because now the efficiency factor is constant and all of the variation is due to the change in the width of the resolution function. In this case we assume that x represents only the dimension perpendicular to the plane. This means that the resolution function is already integrated over all three dimensions in the 'plane', or in other words that the resolution function is projected (see Section 6) onto an axis perpendicular to the plane.

We are interested in the value of G at x, where x is assumed to be the intersection with the plane, while the instrument is at a nominal position x_0. The width η_1 of G depends on x_0. Expanding equation (25) in a Taylor series [with respect to η_1 around η_{10} (at $x=x_0$)] gives

$$G(x-x_0,\eta_1) = G(x-x_0,\eta_{10}) + \eta_2 \times \exp\left\{-\frac{(x-x_0)^2}{2\eta_{10}^2}\right\} \frac{(x-x_0)^2}{\eta_{10}^3}(\eta_1-\eta_{10}) + \ldots \quad (26)$$

For small $(\eta_1-\eta_{10})$ we now obtain $G(x-x_0,\eta_1)$ for a scan which changes the nominal position x_0. The variation of η_1 with x_0 is not of particular interest in this context. Fig. 4 shows $G(x-x_0,\eta_1)/G(x-x_0,\eta_{10})$ as a function of η_1. At the position $x-x_0=\eta_{10}$

$$\frac{G(\eta_{10},\eta_1)}{G(\eta_{10},\eta_{10})} = 1+\frac{\eta_1}{\eta_{10}}-1 = \frac{\eta_1}{\eta_{10}}\,. \quad (27)$$

In Fig. 4 the result of applying equation (27) appears as the broken line. It can be seen that equation (27) agrees with equation (26) at $x-x_0=0$, and $x-x_0=\pm\eta_{10}$, *i.e.* at positions where $G(x,\eta_{10})$ is 1 and 0·61. The broken line is the approximation to the correction obtained by simply dividing by η_1, which is equivalent to dividing by V_1.

Fig. 4 gives the impression that the disagreement between the true correction (the solid line) and the approximate correction (the broken line) is much larger than in fact it is for the four-dimensional resolution function. This is because we have been considering only one dimension. The integration over three dimensions within the plane is already done for every point by the instrument and the approximation there-

fore affects only one of the four dimensions of the resolution function.

The approximation is even better if $\eta_1 \simeq \eta_2$ (*i.e.* $V_I \simeq V_F$), because the change in the width is smaller. The variation of η_1 will now affect both the width and the efficiency factor, and the change in the efficiency factor will be exactly taken into account by $V_I \cdot V_F$ as was shown above.

Thus, for well defined phonons the method of dividing every measured point by $V_I \cdot V_F$ is a good way to obtain data which represent a convolution of the phonon scattering law with a normalized resolution function (see Section 6).

A monitor with a $\frac{1}{k_I}$ characteristic, set in the incident monochromatic beam to control the counting time, directly corrects for the variation of V_I. Hence, for cases 5*a* and 5*b* with k_F fixed and a $\frac{1}{k_I}$ monitor, no corrections for changing resolution are necessary.

6. Discussion of the data corrected by the normalization

In Section 5 we discussed how the normalization of the resolution function affects the intensity of each measured point. Now we will consider the measured widths and integrated intensities in more detail.

To do this, we will first show an interesting property of Gaussian functions for a two-dimensional example. This is most easily understood by imagining that x is a coordinate perpendicular to the plane representing $S(\mathbf{Q},\omega)$ and y stands for the three coordinates in the plane, as was done in Section 5. We mentioned there that the instrument performs an integration within the plane, *i.e.* along y. If we assume $S(\mathbf{Q},\omega)$ to be constant, the integration can be performed over the resolution function alone for every x.

$$\int \exp\left\{-(a_{11}x^2+2a_{12}xy+a_{22}y^2)\right\}\mathrm{d}y = \text{const.}\exp\left\{-\frac{a_{11}a_{22}-a_{12}^2}{a_{22}}x^2\right\}. \quad (28)$$

At $x^2 = \frac{a_{22}}{a_{11}a_{22}-a_{12}^2}$ the probability has dropped to e^{-1} of the probability at $x=0$.

Now we compare the result of the above integration with the result of projecting the ellipse

$$a_{11}x^2+2a_{12}xy+a_{22}y^2=1 \quad (29)$$

onto the x axis. We set $\frac{\mathrm{d}x}{\mathrm{d}y}=0$ and calculate the coordinate x_p and find

$$x_p^2 = \frac{a_{22}}{a_{11}a_{22}-a_{12}}. \quad (30)$$

Thus we see that a projection gives the same width as an integration. This holds for more than two dimensions as well.

Using the projection of the ellipse helps to visualize the factors affecting the measured intensity and line shape. In a scan, in which $\mathbf{Q}_0$ and ω_0 vary, we define ellipsoids of different probabilities, so that for each value of $\mathbf{Q}_0,\omega_0$ one ellipsoid just contacts the plane representing $S(\mathbf{Q},\omega)$ at $\mathbf{Q}_t,\omega_t$ (see Fig. 5). A scan perpendicular to the plane yields the smallest measured width.

Under the assumption that $S(\mathbf{Q},\omega)$ is constant, the probability associated with the 'ellipsoid of contact' times S gives the measured intensity also, the measured width for any direction of scan is larger than the smallest width by a factor $\frac{1}{\cos\varphi}$ (φ being the angle between the scan and the normal to the plane). As long as S is constant, a 'perpendicular' scan will not reveal more physical information than an inclined one.

A more realistic $S(\mathbf{Q},\omega)$ varies with $\mathbf{Q}$ and ω. Then to a good approximation, $S(\mathbf{Q}_t,\omega_t)$ at the contact point can be considered as giving the 'mean value' of $S(\mathbf{Q},\omega)$, which contributes to the scattering at a nominal setting, $\mathbf{Q}_0,\omega_0$ (see Fig. 5). Therefore, the counting rate at $\mathbf{Q}_0,\omega_0$ is $S(\mathbf{Q}_t,\omega_t)$ times the probability on the surface of the contacting ellipsoid. For most scans $\mathbf{Q}_t,\omega_t$ will change with the variation of $\mathbf{Q}_0,\omega_0$. At the position of maximum overlap between $\mathbf{S}$ and $\mathbf{R}$ it follows that $\mathbf{Q}_t=\mathbf{Q}_0$ and $\omega_t=\omega_0$.

We understand that the 'mean value' of $S(\mathbf{Q},\omega)$ described above will change during a scan varying $\mathbf{Q}_0,\omega_0$. If $S(\mathbf{Q},\omega)$ is known approximately, one can

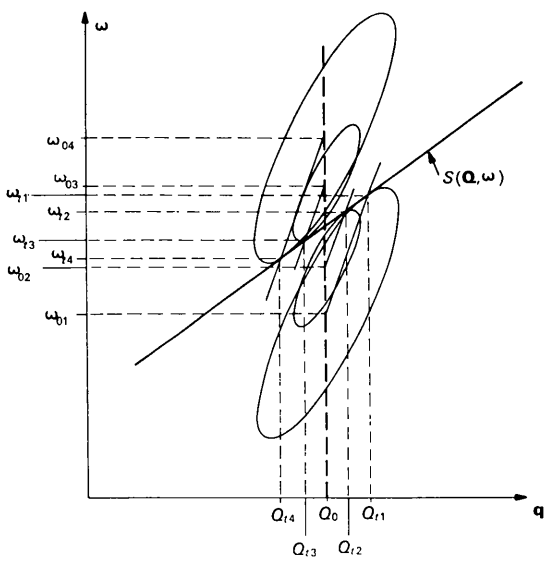

Fig. 5. The ellipses represent projections of four-dimensional ellipsoids for different probability. For a const-Q_0 scan the Q_{ti},ω_{ti} of contact with the scattering law $S(Q,\omega)$ are shown for four different ω_{0i}. Note that the lines connecting $Q_0\omega_{0i}$ with Q_{it},ω_{ti} are parallel.

evaluate the values of $\mathbf{Q}_t, \omega_t$ and take into account the varying 'mean value' of $S(\mathbf{Q},\omega)$. This correction has been performed for phonon measurements in argon (Dorner & Egger, 1971) and in CD_4 (Press, Dorner & Stiller, 1971). For $S(\mathbf{Q},\omega)$ described by a plane, all $\mathbf{Q}_t, \omega_t$ along the scan lie on a straight line through the center of R. Having taken into account both the 'mean value' of S and the normalization corrections explained in Section 5, the unfolding reduces to a one-dimensional problem even if the phonon has an intrinsic line shape, since the contribution of the resolution to the measured width is known. A favourable scan is a scan which has the same $\mathbf{Q}_t, \omega_t$ for all $\mathbf{Q}_0, \omega_0$.

Consider now the measured intensities $I(\mathbf{Q}_0,\omega_0)$ corrected by $V_I[k_I(\mathbf{Q}_0,\omega_0)]$ and $V_F[k_F(\mathbf{Q}_0,\omega_0)]$. We rewrite equation (9)

$$\frac{I(\mathbf{Q}_0,\omega_0)}{V_I \cdot V_F} = \frac{J(\mathbf{Q}_0,\omega_0)}{V_I \cdot V_F} \cdot \Delta t = A \cdot \Delta t \int S(\mathbf{Q},\omega) \times \frac{R(\mathbf{Q}-\mathbf{Q}_0,\omega-\omega_0)}{V_I \cdot V_F} \, \mathrm{d}^3Q\mathrm{d}\omega \quad (31)$$

where Δt is the measuring time which is assumed to be the same for each point. Since $R(\mathbf{Q}-\mathbf{Q}_0, \omega-\omega_0)$ depends on the zero points $\mathbf{Q}_0$ and ω_0, an integration of equation (9) over $\mathbf{Q}_0$ and ω_0 would not be easy. But, $\frac{R(\mathbf{Q}-\mathbf{Q}_0,\omega-\omega_0)}{V_I \cdot V_F}$ is a normalized function independent of $\mathbf{Q}_0$, ω_0 within the approximation discussed in 5*b*. Since this integral is independent of $\mathbf{Q}$ and ω, we integrate equation (31) over $\mathrm{d}\mathbf{Q}_0 \cdot \mathrm{d}\omega_0$ and get

$$\int \frac{I(\mathbf{Q}_0,\omega_0)}{V_I \cdot V_F} \mathrm{d}\mathbf{Q}_0\mathrm{d}\omega_0 = A \cdot \Delta t \cdot \int S(\mathbf{Q},\omega)\mathrm{d}^3Q\mathrm{d}\omega \, . \quad (32)$$

Equation (32) shows us that the integration (effectively a summation) over the corrected intensities yields the integral over the scattering law.

Hence $\frac{I(\mathbf{Q}_0,\omega_0)}{V_I \cdot V_F}$ is a folding of $S(\mathbf{Q},\omega)$ with a resolution function normalized to unity. The unfolding of a Gaussian with $S(\mathbf{Q},\omega)$ will not be further discussed here.

7. Conclusion

We have derived an exact normalization of the resolution function and have shown that the so-called efficiency factor R_0 can be expressed as a function of the normalization and the widths in the direction of the principal axes. This simple result for R_0 should be a great help for numerical evaluation of the folding of the resolution function with the scattering law.

Assuming that $S(\mathbf{Q},\omega)$ varies linearly over the volume of R (at least with respect to three dimensions) we give a method for correcting the measured data without numerical convolution. In the case of phonons it is necessary to assume that $S(\mathbf{Q},\omega)$ is planar to apply this technique. In this case, we show that the unfolding of the data reduces to a one-dimensional problem and the integral over the corrected data yields the integral over the scattering law.

The author has benefited from many discussions with Dr G. Shirane and especially with Dr J. D. Axe. He is indebted to Drs L. Passell and O. W. Dietrich for their careful reading and help with the manuscript.

APPENDIX

Starting with Cooper & Nathans's (1967) equation (6) we find

$$p_i(\mathbf{k}_i) \cdot \mathrm{d}k_{ix} \cdot \mathrm{d}k_{iy} \cdot \mathrm{d}k_{iz} = P_M(k_I)P_{0M} \times \exp\left\{\tfrac{1}{2}\left[\left(\frac{(\Delta k_i/k_I)\tan\theta_M + \gamma_1}{\eta_M}\right)^2 + \left(\frac{2(\Delta k_i/k_I)\tan\theta_M + \gamma_1}{\alpha_0}\right)^2 + \frac{\gamma_1^2}{\alpha_1^2} + \left(\frac{1}{4\sin^2\theta_M\eta_M'^2 + \beta_0^2} + \frac{1}{\beta_1^2}\right)\delta^2\right]\right\} \times \mathrm{d}(\Delta k_i) \cdot k_I \cdot \mathrm{d}\gamma_1 \cdot k_I\mathrm{d}\delta_1 \quad (33)$$

where $\mathrm{d}(\Delta k_i)$ is the component in the direction of $\mathbf{k}_I$, $k_I \cdot \mathrm{d}\gamma_1$ is the component in the scattering plane perpendicular to k_I and $k_I \cdot \mathrm{d}\delta_I$ is the component perpendicular to the scattering plane.

Equation (6) of Cooper & Nathans contains several minor errors. First, the denominator of the δ_1 and δ_2 expressions should contain $\sin\theta_M$ and $\sin\theta_A$ instead of $\tan\theta_M$ and $\tan\theta_A$. Second, they include only one P_o, which is derived in their Appendix I for the monochromator; a similar expression for the analyzer is missing.

There is a more serious objection to their expression for P_o, as given in their equation (24). If we assume $\beta_1 \gg \beta_0$ and η_M', then all incoming neutrons with vertical divergence defined by β_0 must be reflected by the monochromator. To understand how this comes about, we note that the attenuation produced by the finite reflectivity of the monochromator is expressed by P_M [actually $P_M(k_I)$]. The vertical collimation plays no role in determining the values of k_i, which will be reflected; this is entirely determined by the horizontal Bragg condition. Thus, if $P_M(k_I)$ is set equal to unity, we should expect that the integral over δ_1 is proportional to β_0 or in other words that every neutron with an acceptable k_i and a vertical divergence within β_0 will be reflected. In fact, this condition is not satisfied if Cooper & Nathans's formula (24) is integrated. This consistency consideration has been used to derive correct expressions for P_{0M} and P_{0A}, which are

$$P_{0M} = \frac{\beta_0}{\sqrt{4\sin^2(\theta_M)\eta_M'^2 + \beta_0^2}}, \qquad P_{0A} = \frac{\beta_3}{\sqrt{4\sin^2(\theta_A)\eta_A'^2 + \beta_3^2}} \, . \quad (34)$$

Chesser (1971) has pointed out that this error is a consequence of the fact that Cooper and Nathans's equation (14), which describes the probability of vertical broadening of the beam by reflexion from a crystal with a vertical mosaic spread, is not normalized. Equation (C & N 14) should read

$$P(\delta_1-\delta_0)=\frac{1}{\sqrt{(2\pi)}\cdot 2\sin\theta_M\eta'_M}\exp\left\{-\tfrac{1}{2}k_I^2\left(\frac{\delta_1-\delta_0}{Q_M\cdot\eta'_M}\right)^2\right\}. \quad \text{(C \& N 14)}$$

We used the Bragg equation $2\cdot k_I\cdot\sin\theta_M=Q_M$.

The correct P_{0M} consequently reads

$$P_{0M}=\frac{1}{\sqrt{(2\pi)}\cdot 2\sin\theta_M\eta'_M}\cdot P_{0C\&N} \qquad (35)$$

where $P_{0C\&N}$ is given by Cooper and Nathans's equation (24).

Comparing our P_{0M} with equation (5.3) of Tucciarone *et al.* (1971) we found a misprint in their equation (5.3), as a factor $2\pi\cdot\eta'_M\cdot\eta'_A$ is missing in the denominator. Integrating equation (33) we get

$$V_I=P_M(k_I)\cdot(2\pi)^{3/2}\times$$
$$\tan\theta_M\cdot\left[\left(\frac{1}{\eta_M^2}+\frac{4}{\alpha_0^2}\right)\left(\frac{1}{\eta_M^2}+\frac{1}{\alpha_0^2}+\frac{1}{\alpha_1^2}\right)-\left(\frac{1}{\eta_M^2}+\frac{2}{\alpha_0^2}\right)^2\right]^{1/2}$$
$$\times\frac{\beta_0}{\sqrt{(4\sin^2(\theta_M)\eta'^2_M+\beta_0^2)}}$$
$$\times\frac{1}{\sqrt{\left(\frac{1}{4\sin^2(\theta_M)\eta'^2_M+\beta_0^2}+\frac{1}{\beta_1^2}\right)}}\cdot k_I^2\cdot \qquad (36)$$

This reduces to

$$V_I=P_M(k_I)\cdot(2\pi)^{3/2}\cdot k_I^3\cot\theta_M$$
$$\times\frac{\beta_0\cdot\beta_1}{\sqrt{(4\sin^2(\theta_M)\eta'^2_M+\beta_0^2+\beta_1^2)}}\cdot\frac{\eta_M\alpha_0\alpha_1}{\sqrt{(\alpha_0^2+\alpha_1^2+4\eta_M^2)}}\cdot \qquad (37)$$

A similar expression can also be derived for the analyzer, where $P_A(k_F)$ represents the counter efficiency and the reflectivity of the analyzing crystal.

References

ALS-NIELSEN, J., AXE, J. D. & SHIRANE, G. (1971). *J. Appl. Phys.* **42**, 1666.

AXE, J. D., DORNER, B. & SHIRANE, G. (1971). *Phys. Rev. Letters*, **26**, 519.

BAUER, K. H. W., JAGODZINSKI, H., DORNER, B. & GRIMM, H. (1971). *Phys. Stat. Sol.* **48**b, 437.

BJERRUM MØLLER, H. & NIELSEN, M. (1970). *Instrumentation for Neutron Inelastic Scattering Research*, p. 49–76. Vienna: IAEA.

CHESSER, N. (1971). Private communication.

COLLINS, M. F. (1963). *Brit. J. Appl. Phys.* **14**, 805.

COOPER, M. J. & NATHANS, R. (1967). *Acta Cryst.* **23**, 357.

DIETRICH, O. W. (1971). *Resolution determined by Monte Carlo calculation*, to be published.

DORNER, B. (1971). *J. Appl. Cryst.* **4**, 185.

DORNER, B. & EGGER, H. (1971). *Phys. Stat. Sol.* **43***b*, 611.

HUTCHINGS, M. T. & SAMUELSEN, E. J. (1970). Unpublished.

HUTCHINGS, M. T., SHIRANE, G., BIRGENEAU, R. J. & HOLT, S. L. (1972). *Phys. Rev.* **B5**, 1999.

KOMURA, S. & COOPER, M. J. (1970). *Japan J. Appl. Phys.* **9**, 866.

LAU, H. Y., CORLISS, L. M., DELAPALME, A., HASTINGS, J. M., NATHANS, R. & TUCCIARONE, A. (1970). *J. Appl. Phys.* **41**, 1384.

MAIER-LEIBNITZ, H. (1966). *Nukleonik*, **8**, 61.

NIELSEN, M. & BJERRUM MØLLER, H. (1969). *Acta Cryst.* A**25**, 547.

PRESS, W., DORNER, B. & STILLER, H. H. (1971). *Solid State Commun.* **9**, 1113.

SAMUELSEN, E. J. (1971). In *Structural Phase Transitions and Soft Modes*, by E. J. SAMUELSEN, E. ANDERSEN & J. FEDER. Oslo: Universitetsforlaget.

SAMUELSEN, E. J., HUTCHINGS, M. T. & SHIRANE, G. (1970). *Physica*, **48**, 13.

SHIRANE, G. (1971). Private communication.

STEDMAN, R. (1968). *Rev. Sci. Instrum.* **39**, 878.

STEDMAN, R. & NILSSON, G. (1966). *Phys. Rev.* **145**, 492.

TUCCIARONE, A., LAU, H. Y., CORLISS, L. M., DELAPALME, A. & HASTINGS, J. M. (1971). *Phys. Rev.* B**4**, 3206.

WERNER, S. A. (1971). Private communication.

WERNER, S. A. & PYNN, R. (1971). *J. Appl. Phys.* **42**, 4736.